A Hyperspectral-Physiological Phenomics System: Measuring Diurnal Transpiration Rates and Diurnal Reflectance

Shahar Weksler [1,2,*], Offer Rozenstein [2], Nadav Haish [3], Menachem Moshelion [3], Rony Walach [4] and Eyal Ben-Dor [1]

1   Porter School of Environment and Earth Sciences, Faculty of Exact Sciences, Tel Aviv University (TAU), Tel Aviv 6997801, Israel; bendor@tauex.tau.ac.il

2   Institute of Soil, Water and Environmental Sciences, Agricultural Research Organization, Rishon LeZion 7528809, Israel; offerr@volcani.agri.gov.il

3   The Robert H Smith Institute of Plant Sciences and Genetics in Agriculture, The Hebrew University of Jerusalem, Rehovot 7610001, Israel; nadav.haish@mail.huji.ac.il (N.H.); menachem.moshelion@mail.huji.ac.il (M.M.)

4   Department of Soil and Water Sciences, The Robert H. Smith Faculty of Agriculture, Food and Environment, The Hebrew University of Jerusalem, Rehovot 76100, Israel; rony.wallach@mail.huji.ac.il

*   Correspondence: weksler@mail.tau.ac.il; Tel.: +972-3-640-5679

check for updates

Abstract: A novel hyperspectral-physiological system that monitors plants dynamic response to abiotic alterations was developed. The system is a sensor-to-plant platform which can determine the optimal time of day during which physiological traits can be successfully identified via spectral means. The directly measured traits include momentary and daily transpiration rates throughout the daytime and daily and periodical plant weight loss and gain. The system monitored and evaluated pepper plants response to varying levels of potassium fertilization. Significant momentary transpiration rates differences were found between the treatments during 07:00–10:00 and 14:00–17:00. The simultaneous frequently measured high-resolution spectral data provided the means to correlate the two measured data sets. Significant correlation coefficients between the spectra and momentary transpiration rates resulted with a selection of three bands (ρ523, ρ697 and ρ818nm) that were used to capture transpiration rate differences using a normalized difference formula during the morning, noon and the afternoon. These differences also indicated that the best results are not always obtained when spectral (remote or proximal) measurements are typically preformed around noon (when solar illumination is the highest). Valuable information can be obtained when the spectral measurements are timed according to the plants' dynamic physiological status throughout the day, which may vary among plant species and should be considered when planning remote sensing data acquisition.

Keywords: hyperspectral; remote sensing; phenomics; sensor-to-plant; functional phenotyping; water stress

1. Introduction

Global environmental changes, together with the constantly rising world population, present complex challenges to food security [1]. It is estimated that, by 2050, the world population will exceed nine billion people [2]. To withstand these challenges, agricultural production must keep up with this trend to sustain human life. It is therefore desirable to select specific genes in crops that ensure better food security, as well as the best phenotype from that genetic line, to be bred or planted.

The rapid development of genomic technologies over the past decade has assisted the progress of complete genome sequencing. Many of these genes offer desirable traits and can fulfill specific roles.

However, the lack of high-throughput phenotyping tools has created a bottleneck in crop breeding [3–5]. This has resulted in difficulty when selecting the best candidate crops for reproduction. During the past few years, considerable attention has been given to this subject. Plant phenomics is defined as "the study of plant growth, performance, and composition" [1]. Phenotypes, such as improved yield and growth rates, pest resistance, and abiotic stresses have therefore become the main focal point for phenomics systems designed to select the best plants with the desired phenotype. While manually measuring these attributes can be a tedious and time-consuming task on a plant-by-plant basis in a greenhouse or in the field, most phenomics systems are already taking advantage of computer vision and proximal and remote sensing [6–9].

Phenomics systems can roughly be divided into two types: field and greenhouse phenomics. While the sensors that comprise these systems are relatively similar (i.e., RGB camera, multi/hyper spectral camera, broadband thermal camera, LIDAR), the platforms these sensors are embedded on differ greatly. Typically, field phenomics is carried out using ground vehicles or an unmanned aerial vehicle. Several manned and unmanned ground vehicles have been invented in the last decade for this purpose, mainly focusing on maize, wheat, and vines [6–10]. On the other hand, greenhouse phenomics systems are usually constructed with a conveyer belt that transports plants to an imaging chamber [11,12]. In such chambers, plants are illuminated with high-intensity light (e.g., using a halogen lamp) to produce high signal-to-noise (SNR) measurements by the recording instrument. Conditions in a semi-controlled greenhouse are considered to be near-field conditions in terms of environmental factors such as the illumination cycle or the relative humidity. However, one clear advantage of greenhouse facilities is their ability to mimic and control specific abiotic stresses while measuring traits that are difficult to measure in the field, such as continuous plant weight. Nevertheless, such facilities and systems are expensive and the ability to process large quantities of plants depends on the rate of plants entering the imaging chamber. In addition, conveyor belts and imaging chambers are limited by the size of the plant they are able to transport and image. It is therefore preferable to develop a system in which the plants are kept static and the measuring platform is mobile [13].

While many studies exploit RGB imaging for plant phenomics, few have used hyperspectral cameras. Elvanidi et al. [14] used a hyperspectral camera in a growth chamber to track changes to the reflectance of tomato plants under four different water treatments. Pacumbaba and Beyl [15] used a hyperspectral camera and lettuce plants grown in greenhouse conditions to assess the usefulness of hyperspectral techniques in the detection of nutrient stress. They concluded that the spectral data have shown potential as a diagnostic tool. Pandey et al. [12] used a conveyer belt to transfer maize and soybean plants under different water and nutrient deficits to an imaging chamber to image and quantify leaf water content and leaf concentrations of macronutrients. The authors determined that hyperspectral imaging is potentially useful as a high-throughput phenotyping tool, but future research is needed.

In addition, currently, most imaging sensors in space measure the earth at an approximately constant time, whereas sensors on airborne platforms are mostly operating during high sun illumination. The disadvantage of a single daily image at a given time with respect to plant diurnal changes has been recognized by the ecosystem space-borne thermal radiometer experiment on a space station (ECOSTRESS) mission, which is already in orbit [16]. ECOSTRESS is taking several thermal images of the earth per day in selected areas to analyze plant responses to the diurnal water cycle in the soil and atmosphere. Moreover, in their review, Roitsch et al. [13] emphasize the importance of the temporal resolution: while current phenomics platforms take images of plants once a day, their reaction to abiotic changes such as radiation and atmospheric water content cause rapid changes in stomata aperture and chlorophyll allocation in the leaf [17,18]. Abiotic changes, such as changes to the soil water content or water content in the atmosphere, manifest themselves by alteration to the plant momentary transpiration rate and may be revealed by direct measurements using a leaf gas exchange chamber [5].

In a similar fashion, it is apparent that most of the airborne (man and unmanned) remote sensing data acquisition takes place close to midday, as high solar irradiance assures a high SNR and minimizes shading effects. In this case, the diurnal physiological variations of the plants are neglected in order to ensure better illumination conditions, but this neglection may result in the under sampling of diurnal variations and misdetection of physiological phenomena that would be revealed during different hours of the day. It is therefore desirable to image plants multiple times during the day, along with continuous physiological measurements, in order to analyze hourly plant changes and responses to their surroundings.

Moreover, although the aforementioned field and greenhouse phenomics systems have produced a great deal of data, they lack the ability to combine continuous in situ whole-plant physiological measurements with hyperspectral images. To address the requirement for a low cost, high-throughput phenotyping method, the objective of this study was to develop an automated imaging phenotyping platform combining hyperspectral images with continuous physiological measurements.

We describe a new greenhouse phenotyping system, which combined the PlantArray (PA) 3.0 functionality (www.plant-ditech.com) with a customized push broom spectral imaging system that moves over the plants, imaging dozens of plants in the experimental array at a time at high spectral and spatial resolutions. PA 3.0 is a whole-plant physiological measuring system, so the gathered spectral data is analyzed per plant, by the mean plant spectral signal and its corresponding physiological response. With respect to published literature, this is the first attempt to produce multiple diurnal greenhouse measurements using a moving hyperspectral camera, natural light, and static plants that are continuously monitored by a physiological measurement system (PA). As a demonstration, the system was evaluated through the case study of an experiment conducted on pepper plants receiving different potassium treatments. Potassium is considered an essential macro-nutrient for plants. However, it lacks direct absorption features in the visible and near infrared (VIS-NIR) portion of the electromagnetic spectrum [12]. The combined ability of both systems for continuous monitoring was harnessed to track secondary changes to spectrum and relate spectral diurnal changes to physiological attributes. The ability to track changes to the reflectance spectral curve of plants as a consequence of different potassium treatments was used to show that the optimal time for data fusion and analysis must be accounted for.

2. Materials and Methods

2.1. PlantArray

The PA 3.0 platform is a whole-plant functional phenotyping system that controls the fertigation of every individual plant connected to its main controller [5,18]. In addition, the system calculates and logs plant-specific physiological attributes based on their continuous weight measurements. Each plant is placed in a load-cell that acts as a weighing lysimeter coupled with a closed-circuit electronic board controlling and logging weight measurements. The system is composed of an array of plants randomly distributed on a growing table in the greenhouse and the weight of each plant is logged every three minutes. A detailed experimental setup is described in [18,19]. Briefly, the load-cells were occupied with pots containing an inert substance (quartz sand). The pots were placed in a special plastic container which restricts drainage to a selected degree. Evaporation was restricted using a plastic cover with a hole in its center for the plant stem to emerge through, thus limiting the changes in pot weight to the effect of plant transpiration (Figure 1).

Repeated water irrigations during the night were intended to wash the previous residues from the irrigation system before irrigating specific pots with a desired treatment. Before dawn, the system automatically irrigated the pots with the selected treatment using four drippers for an even water distribution. The last irrigation pre-dawn contained the specific solution treatment that each individual plant was to receive.

Figure 1. A pot in the greenhouse. Four drippers provided the water and nutrients, while evaporation was restricted with a plastic cover. The pot was loaded onto a green plastic container that collected a predetermined amount of drainage. The pot and plastic container were placed on a scale which is connected to Plantarray 3.0 system.

Using this approach, the plant daily weight, daily growth, and daily transpiration are calculated by the system for each sample. The plant daily weight is calculated by averaging ten measurements after the last irrigation when the drainage has finished and normalizing them by removing the initial pre-planting pot weight. Daily biomass growth is calculated as the difference between two daily weights, pre-dawn. Daily transpiration is calculated as the weight difference between two consecutive irrigations. Momentarily transpiration rate (TR) is associated with weight decrease throughout the daytime and is calculated by the first derivative of two consecutive weight measurements [18].

2.2. Experimental Setup

72 pepper seedlings (*Capsicum annuum* variant Rita) were sown under controlled conditions and planted in 3.9 L pots approximately four weeks post-germination. The plants were grown during 31 March–5 May, 2019; however, images were captured only until 15 April because of canopies overlap between adjacent plants that occurred after that time and which made the analysis of individual plants difficult. The temperature and humidity in the greenhouse were logged by the PA system. Pots were filled with sandy (quartz) soil, and their initial weight with and without the plants was measured to calculate the plant starting weight.

During the experiment, the temperature was kept under 35 °C by blowing moist air through vents in the north wall of the greenhouse (the sun travels through the south). The temperature and relative humidity ranged between 20 and 35 °C and 26% and 90% respectively, with low values during the night. Three different potassium treatments were administrated using Plant-array's computerized irrigation on a special experimental table (D-table) in the greenhouse: Low (L), Medium (M), and high (H) levels of potassium. Every pot in the 72-pots array was attributed to a treatment group using a completely randomized approach (Table 1). The medium amount of potassium (M) was determined based on different recommendations from three different fertilizing companies +10% (105 PPM, 2.69 mM). The additional treatments were 70% surplus (H, 180 PPM, 4.6 mM) and 30% deficit (L, 30 PPM, 0.77 mM). On the final day of the experiment, the plants were removed from their pots for root examination. Varying degrees of root fungi were discovered, ranging from very lite to very harsh infections. After careful examination, it was decided to exclude all infected plants from further analysis. Seventeen samples from the medium treatment, 15 from the low potassium treatment, and 13 from the high potassium treatment were removed from the analysis resulting with 7, 10 and 11 samples for the medium, low and high treatments, respectively. While the greenhouse setup allows for hourly comparison, it is more practical and robust to split the daytime into three temporal groups. Based on the TR daily cycle and differences the database was naturally averaged into the following three periods: morning (07:00–10:00) when TR increased, noon (11:00–13:00) when TR peaked and afternoon (14:00–17:00) when TR decreased.

Table 1. Randomly distributed treatments on the experimental table.

	1	2	3	4	5	6	7	8	9	10	11	12	13	14	15	16	17	18
D	L	L	M	M	L	M	L	M	H	L	L	M	M	L	M	L	M	H
C	M	H	H	L	H	L	M	H	L	M	H	H	L	H	L	M	H	L
B	L	L	M	H	M	H	L	M	M	L	L	M	H	M	H	L	M	M
A	M	H	H	M	H	L	H	L	H	M	H	H	M	H	L	H	L	H

L: potassium deficit, M: medium level, H: potassium surplus. The number of plants in each group was 24. Grayed cells represent root fungi disease.

2.3. The Automated Sensor-to-Plant Imaging System

The system was developed in a semi-commercial greenhouse located at the Faculty of Agriculture, Food and Environment in Rehovot, Israel. The roof and side panels of the greenhouse are made from a clear PVC material that diffuses the incoming natural light. With the intention of keeping the cost at a minimum, we modified and installed a mobile irrigation system (IRMO11, Urbinati.com, Italy) to a sensor carrier platform attached to the ceiling of the greenhouse in order to move the camera over the table at a constant speed. The mobile platform was built from lightweight materials and supported by the greenhouse infrastructure, without any structural changes, allowing it to span the entire length of the greenhouse (25 m). The platform was attached with fasteners, bolts, and cables, and built within a few hours. A small laptop controlled the camera and collected the data. A microcontroller connected to the laptop was programmed to run the platform every hour during the day (Figure 2). The overall cost of the moving platform, computer and hyperspectral camera is approximately 25,000 USD. Special attention was given to the camera and laptop as they were situated at the ceiling of the greenhouse, where the temperature and relative humidity can reach 45 °C and 92%, respectively. To address this, an additional cooling fan was placed under the computer, far away from the canopy, as well as a large protective polystyrene sheet. In addition, the camera was kept turned on, to avoid inner condensation on the lens.

Unlike other field vehicles, the system does not cast a shadow on the plants [20], and thus it does not require the use of an artificial light source. The measured signal is therefore the direct representation of diffuse sunlight reflected from the leaves. Furthermore, mechanical vibration may cause physiological artifacts in the growing period [21]. To reduce such effects, in this system, plants are not mechanically disturbed by conveying them to a photographing chamber or other measuring devices, and images are taken without moving the plants.

During the daytime (07:00–17:00, LCT), an image of the plants was captured automatically using a hyperspectral camera, (FX10e, Specim, Finland). The camera is a push-broom sensor, with a spectral range of 400–1000 nm, typically termed VIS-NIR camera (visible 400–700 nm, near infrared 700–1000 nm). The camera was positioned 2 m above the growing table, had 1024 pixels in a line, 448 spectral bands, and a field of view of 38°. The lightweight camera produced an SNR suitable for operation under the diffused natural light conditions in the greenhouse. The camera's focus was manually set to 20 cm above the pot rims and adjusted manually every few days.

Similar to [8,22,23], at the start of each pass, the camera was positioned over a white reference panel (99% reflectance, spectralon, Labsphere Inc. USA) and the exposure time was adjusted to match the current illumination conditions to prevent saturation across all spectral bands. To do so, the exposure time was set to a high value causing saturation in all spectral bands and was lowered incrementally until no saturation was present in all bands in all the pixels of the white reference panel. Once the exposure time was set, the system moved at a constant speed and the camera captured an image of the white reference panel, followed by all the plants, line by line (Figure 3). Once all plants along the table were imaged (12 m, 1.5 min), the system returned to its base position automatically to wait for the next acquisition run. Additionally, although the camera system was automaticaly trigered, it failed to capture images several times during the experiment.
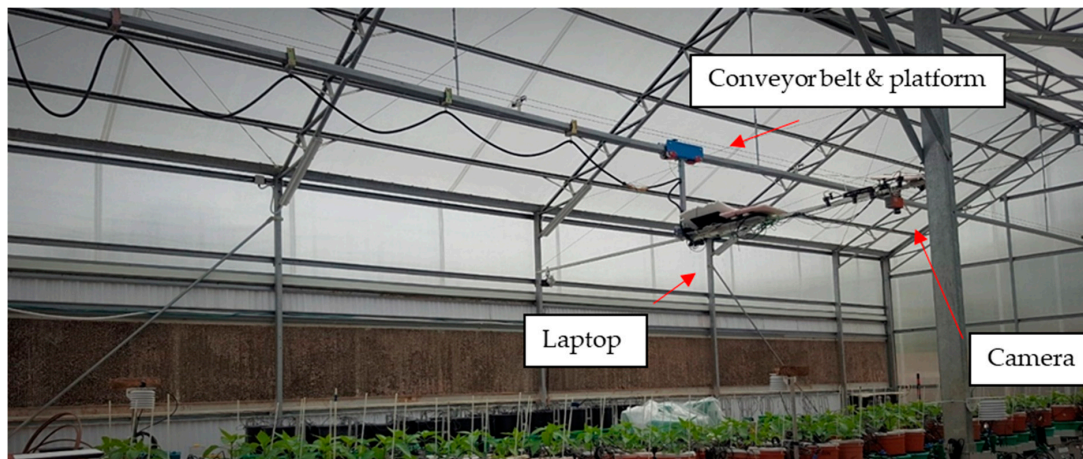
Figure 2. A view of the imaging platform as it moved above the plants. The platform was constructed from lightweight materials and deployed within just a few hours.
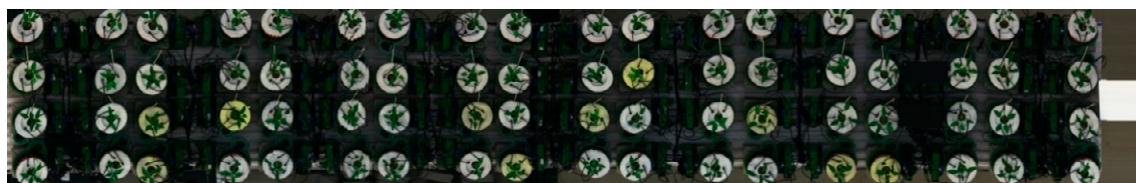

Figure 3. RGB image of 72 pepper plants on a table in the greenhouse. The camera movement was from right to left, starting with the white reference panel for exposure time calibration.

2.4. Whole-Plant Average Spectrum Extraction

Average plant spectra were extracted from each individual plant as shown in Figure 4. Each image was first preprocessed from the raw digital number (*DN*) to reflectance. The *DN* image was initially transformed to radiance units using a gain image produced by the camera's manufacturer and a dark current image acquired with a closed shutter using the following equation:

$$L_{i,j} = \frac{(DN_{i,j} - \overline{DN}_{cs}) \times DN_{gain}}{T} \tag{1}$$

where $L_{i,j}$ is the radiance of pixel i, j; $DN_{i,j}$ represents the raw digital numbers of pixel i, j; $\overline{DN}_{cs}$ is the closed shutter image; DN_{gain} is a gain image produced by the manufacturer by standard calibration protocols and T is the exposure time.
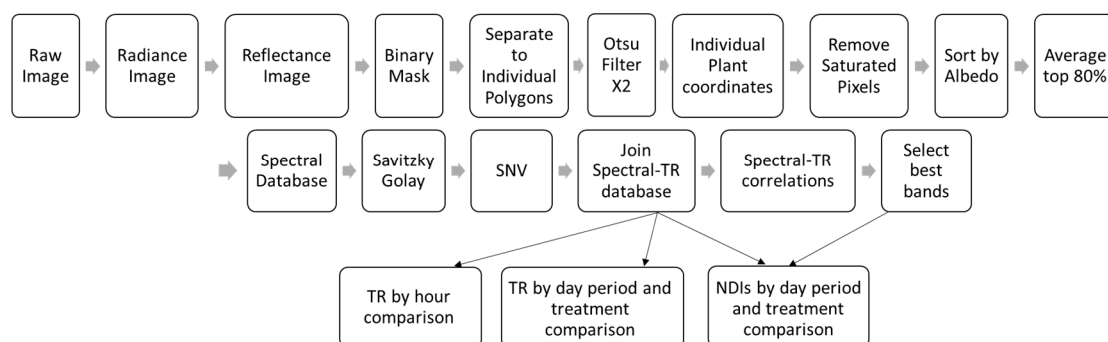

Figure 4. A flow chart summarizing the processing steps of an individual hourly image into 72 plant mean spectra.

Then, the reflectance image was produced using the following equation:

$$\rho_{i,j} = \frac{L_{i,j}}{\overline{L}_{WR}} \tag{2}$$

where $\overline{L}_{WR}$ is the mean radiance spectrum of the white reference panel.

Similar to [12], to separate the green leaves from the background, a binary mask was applied by calculating the first derivative between bands 266 and 209 (752.33 and 673.27 nm, respectively). These specific bands were selected after careful examination to exclude green plastics in the scene which might have been misclassified as green leaves and could not be detected using traditional NDVI. Then, a web of vertical and horizontal lines was drawn around every plant in the image. The intersection of lines around a plant created a polygon bounding box surrounding each plant. For each polygon, a histogram of the values was calculated, and the Otsu filter [24] was used to find the mask value which best separated the green leaves from the background. A second run of the Otsu filter was carried out to separate the leaves' edges which were considered mixed pixels from their centers (Figure 5). The remaining pixel coordinates were logged and used to mask out the background from the leaves. The remaining pixels describing the entire canopy of the plant were then compared using their radiance values against the mean radiance of the white reference panel. Since the exposure time was calibrated to prevent saturation using the white reference panel, pixels with a radiance spectrum higher than the white reference panel were omitted from the analysis. These pixels were usually the results of swift changes in illumination during image acquisition and were less than 5% of the sum of all canopy pixels. The remaining canopy pixels were sorted by their mean albedo (the average reflectance between 400 and 700 nm) and the highest 80% were averaged to a single plant spectrum to exclude shaded pixels and keep only pure pixels.
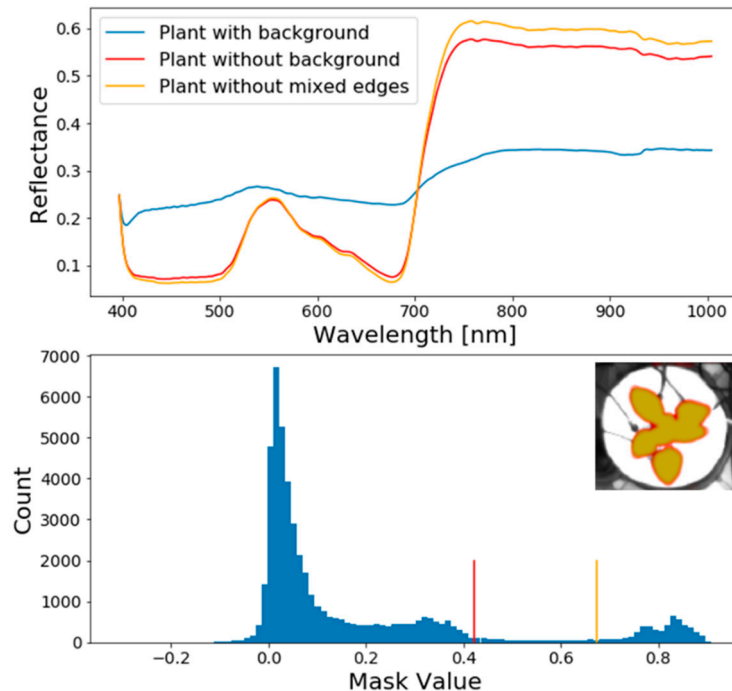

Figure 5. Top: mean spectrum of an exampled plant with its surrounding background (blue), mean spectrum without the background after running Otsu filter (red), mean spectrum of the plant without leaves edges after second Otsu filter run. Bottom: a histogram of the bounding box and the values calculated by Otsu filter.

Finally, the spectra were smoothed using Savitzky–Golay method [25] using a windows size 7 and a 2nd order polynomial, followed by a reduction of scatter effects by standard normal variate (SNV) transformation [26].

The spectral database was joined with the PA measured attributes by the acquisition time. The momentary TR was averaged as ±5 measurements around each image acquisition time. Additionally, the daily transpiration, daily growth and cumulative transpiration were calculated and logged for each plant.

To focus on spectral changes matching the TR grouping (morning, noon, afternoon) and differences correlated to significant TR differences, Pearson correlation coefficients were calculated between the morning, noon and afternoon spectra and with the complimenting TR. The most correlated bands in the VIS, red-edge and NIR (one from each) were selected. Similar to [17], in order to capture the differences between the groups' TR using the spectral information, normalized difference indices (NDI) were calculated using the bands which showed the highest correlation with TR in this setup, and a reference band which showed no correlation. An NDI was calculated as:

$$\text{NDI} = \frac{\rho(\text{ref}) - \rho(\text{corr band})}{\rho(\text{ref}) + \rho(\text{corr band})} \tag{3}$$

where $\rho(\text{ref})$ is the reflectance value of the reference band and $\rho(\text{corr band})$ is the reflectance value of the correlated band selected. Normal distribution tests of the TR and calculated NDI were carried out using the Shapiro–Wilk test. Since not all data were found to be normally distributed the Friedman test for repeated measures was used with a post-hoc Wilcoxon signed ranks test for pairwise comparison using a Bonferroni correction [27]. As these tests require equal sample sizes in each group, in cases of unequal groups, the larger group was randomly reduced to the size of the smaller group prior to database partitioning and averaging. TR differences between the treatment groups were first compared by partitioning the database by the hour and averaging by the treatments for every date (hourly sample sized is depicted in Table 2). The TR were then compared between the day periods (total sample in a day period = 831) by averaging the database by the day period and averaging all the treatment for every date and additionally a within period comparison by further partitioning the former by the average of the treatments (Table 3 depicts total sample sizes). The calculated NDI were compared between the treatment groups of every daily period.

Table 2. The hourly sample sizes.

Hour	7:00	8:00	9:00	10:00	11:00	12:00	13:00	14:00	15:00	16:00	17:00
Samples	49	63	84	77	70	55	91	94	98	84	84

3. Results

3.1. Database Size

The resulting size of the database was 3235 mean plant spectra from 114 images that were captured over 13 days. Low, medium, and high treatments consisted of 1061, 849, and 1325 samples, respectively. The differences in the number of spectra per group are the result of the infected plants elimination. Moreover, changes in illumination after the exposure time was calibrated and during image acquisition caused some plants to be in the shadow or become very bright. These specific plant measurements were omitted from the analysis along with the diseased plants infected by root fungi.

3.2. Plants' Physiological Parameters

No significant daily transpiration and daily biomass gain differences were found between the treatment groups (data not shown). However, the mean TR of the treatment groups per hour (time of image acquisition) over the entire experiment were significantly different (Figure 6). Significant TR differences between the groups were calculated at 7:00–10:00, and 14:00–17:00. During the morning, under low sun radiation conditions, the TR of the plants with a potassium deficit was significantly higher than the two other treatments (medium and surplus, 7:00, 9:00–10:00, and from the medium potassium group at 8:00). As the day progressed and the ambient conditions in the greenhouse changed, the trend changed. No significant differences were found during 11:00–13:00, when TR and sun radiation peaked. At 14:00–15:00, the low treatment was significantly different from the other treatments and at 16:00–17:00, the TR of the low and high treatments were significantly different.
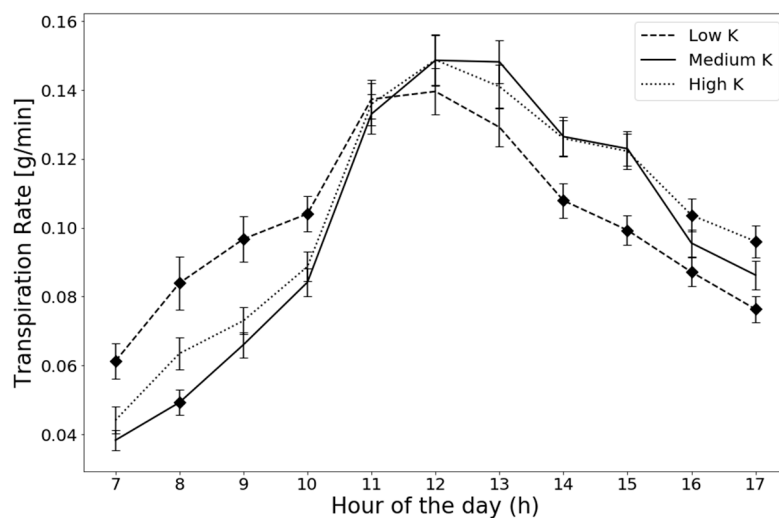

Figure 6. Mean transpiration rates calculated by PlantArray 15 min prior and after every round hour (image acquisition) across all 13 days of the experiment. The transpiration rates follow a daily pattern, reaching maximum transpiration rates at noon. Groups were compared using Friedman test followed by the Wilcoxon signed rank test. Significant differences were calculated at 7:00, 9:00–10:00 and 14:00–15:00 between the low treatment and other treatment groups (marked as a black diamond), at 8:00 between low and medium treatment groups and at 16:00–17:00 between low and high treatment groups.

The grouping to three day-period groups resulted with 1041,831,1363 measurements in the morning, noon and afternoon, respectively and several hundred measurements per treatment (Table 3). Following the grouping, the mean TR was still significantly different between the different daily groups (Figure 7). Next, the database was further partitioned by grouping by the treatment groups. No significant differences were found between the treatment groups during noon. However, during the morning, all the treatment groups were significantly different from one another and during the afternoon the low potassium treatment group was significantly different from the medium and high groups (Figure 7).
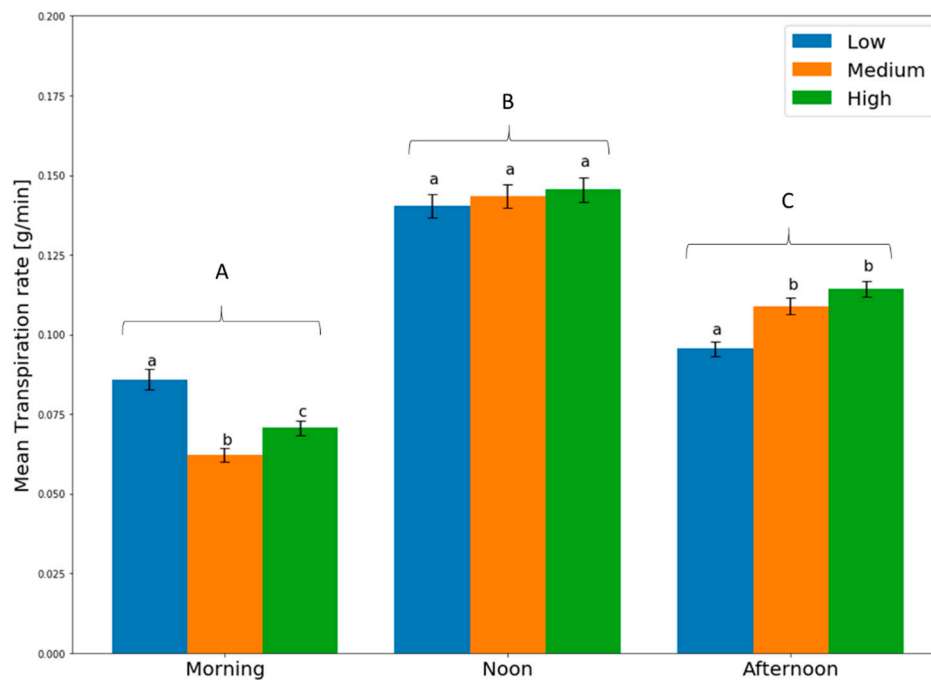
Figure 7. Mean ± SE transpiration rates by the daytime (significant differences are marked with different uppercase letters, A, B, C) and the different treatment groups (high, medium and low levels of potassium fertilization, significant differences are marked with different lowercase letters, a, b, c). Groups were compared using the Friedman test followed by the Wilcoxon signed rank test. Different letters above bars represent significant differences.

3.3. Spectral Database

The combined effect of the time of the day and potassium fertilization on the sample's spectrum was examined by the mean spectrum for each treatment group and day period (Figure 8(A1–A3)). Reflectance variations between the groups are visually witnesed in the VIS as well as in the NIR. However, following the SNV transformation the diurnal spectral difference are drastically reduced (Figure 8(B1–B3)), resulting with a uniform spectra across the day. Small changes in the green bands region (~560 nm) and in chlorophyl absorption bands (460 and 680 nm) are present and the decrease in NIR reflectance is eliminated. Additionaly a sharp absorption feature at ~940 nm followed by a flat absorption feature at ~970 nm belong to the O-H bond 1st overtone absorption feature of water vapor and liquid water [28,29].

Spectral correlations to TR were calculated by the day period to fully exploit the system's ability. The correlations were calculated for each day period individually and their values are presented in Figure 9. Varying values of correlations were calculated for each spectral band and day period. The highest absolute correlations for the all day period was calculated for bands 697, 523 and 818 nm, which indicates that they are more correlative to TR. Additionally, band 760 nm, which is related to the atmospheric O_2-A absorption, showed no correlation to TR and was selected as a reference band. This means that different bands may be used to explore TR alterations during different periods of the day, as an indirect effect of TR and potassium variations on the plants' reflectance.
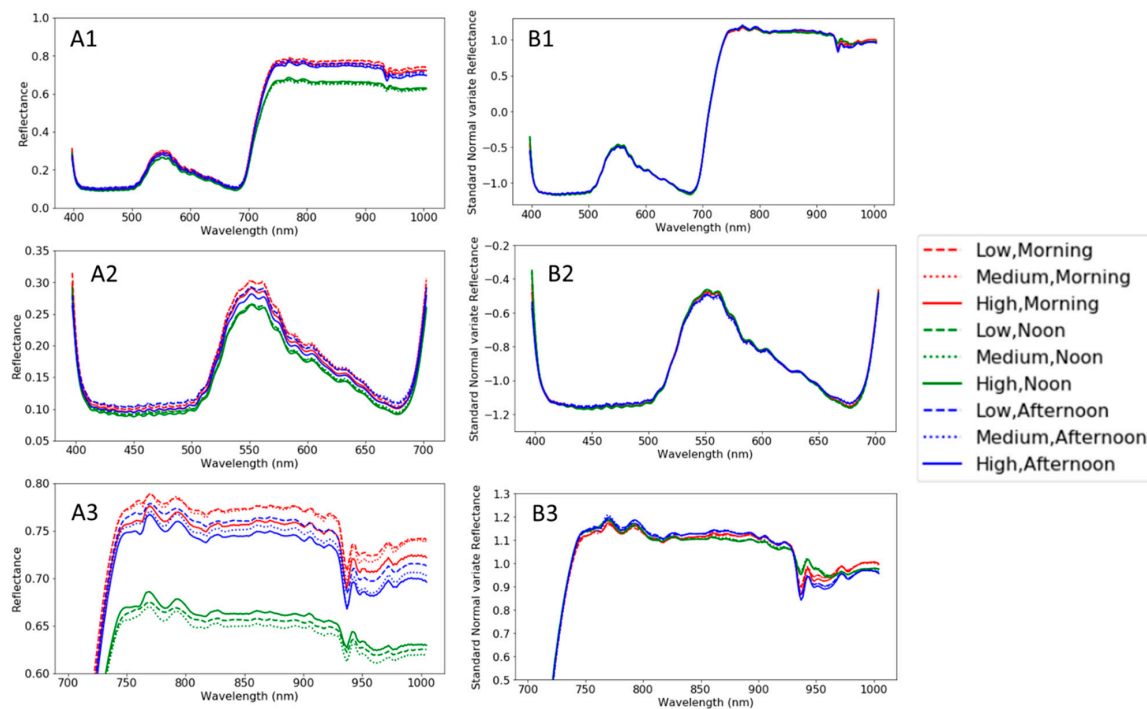
Figure 8. Mean reflectance values of the three treatment groups: potassium deficit (low, dashed line), medium (solid line), and surplus (high, dotted line) during the three day period (morning–red, noon–green and afternoon–blue). (**A1**) entire reflectance region, (**A2**) VIS region reflectnace, (**A3**) NIR region reflectance, (**B1**) entire standard normal variable (SNV) refrlectnce region (**B2**) VIS region SNV, (**B3**) NIR region SNV.

Table 3. Normalized difference indices results for the different day periods and treatment groups.

Day Period	Treatment	(760, 523 nm)		(760, 697 nm)		(760, 818 nm)	
		Value	Sig	Value	Sig	Value	Sig
Morning	Low (n = 273)	6.41	A	5.79	AB	0.023	A
Morning	Medium (n = 273)	6.55	A	5.81	B	0.023	A
Morning	High (n = 273)	6.98	B	6.29	A	0.01	B
Noon	Low (n = 216)	6.38	A	5.93	AB	0.025	A
Noon	Medium (n = 216)	6.54	A	5.94	B	0.025	A
Noon	High (n = 216)	6.96	B	6.31	A	0.018	B
Afternoon	Low (n = 360)	6.44	A	5.92	NS	0.21	A
Afternoon	Medium (n = 360)	6.49	A	5.93	NS	0.2	A
Afternoon	High (n = 360)	6.93	B	6.36	NS	0.01	B

Groups were compared using the Friedman test followed by the Wilcoxon signed rank test; different letters mark significantly different mean values ($p < 0.05$); NS: not significant.

Using these bands and the 760 nm reference band, three different NDI were calculated using Equation (3), and are compared in Table 3. During the morning, all but one NDI combination (523,818 nm) resulted in significantly different values between high levels of potassium and the other two treatment groups. These NDIs also resemble the amount of potassium fertilizer given to the treatment group. One NDI (697 nm) resulted in significantly different values between the high and medium treatments but showed no resemblance to a trend in TR of the treatment groups or the amount of fertilizer. Interestingly, during noon, the same trend in the results were calculated, although TR did not show any significant differences between the groups during that day period. During the afternoon, the high treatment was significantly different from the other two treatments in two NDIs (523,818 nm)

and their values showed the same trend as the TR values. However, NDI (697 nm) was not significantly different between any of the treatment groups.
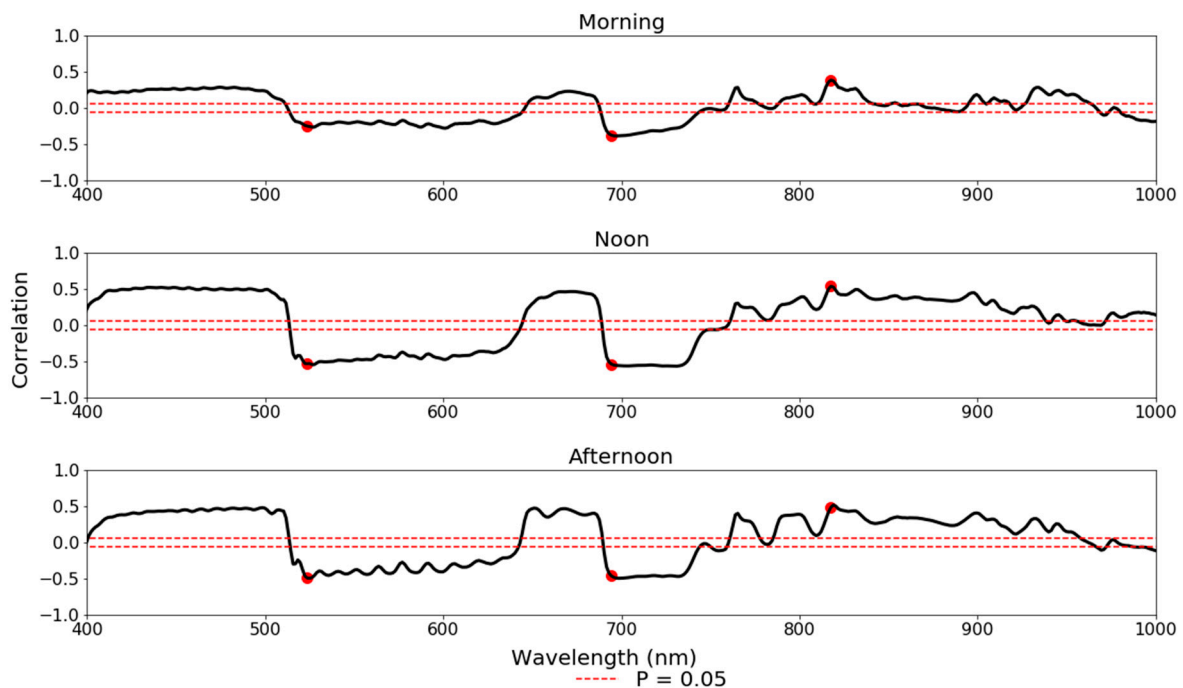

Figure 9. Correlation coefficients between standard normal variate reflectance rates and transpiration rates during the morning (n = 2376), noon (n = 1970) and afternoon (n = 3271). Critical correlation value (confidence level) is marked with a red dashed line; selected maximum absolute correlation bands are marked with a red circle.

4. Discussion

Hyperspectral remote sensing of plants for precision agriculture is typically carried out either from air or space around midday under optimal illumination and minimal shadow conditions, mostly irrespective of the physiological status of the imaged plants. The assumption that the TR is high during this time interval contributes to the conception that this is the preferable time for image acquisition. However, the capability of the hybrid system to monitor plants using hyperspectral images and simultaneously measure TR throughout the day demonstrates that this presumption is not always valid. During noon, TR did not significantly vary between the given potassium treatments, but the calculated NDI were found to be significantly different between the groups. This contradiction between the direct and remote measurements underlies the significant difference of the NDI. If spectral measurements were only carried out during noon, the results of those measurements would be misleading and counterproductive. During the morning and the afternoon, the calculated narrow band indices (523, 818 nm) were significantly different between low and high levels of potassium, which is in agreement with the real TR. However, these indices also showed high and medium levels differences (which is not true for the afternoon's TR values) and no difference between low and medium during the morning (which is present in the morning's TR values). Therefore, this system seems more sensitive to extreme differences (low and high potassium fertilization) and not moderate differences (low and medium or medium and high). Moreover, while the NDIs were calculated based on correlated bands to TR, their calculated values were not in full agreement with the diurnal cyclic pattern of TR and treatment effect. During the morning NDIs (523 and 697 nm) show a trend corresponding to potassium amounts and not its effect on TR, and NDI (818 nm) did not follow any trend in TR or potassium amounts. Nonetheless, during the afternoon, NDIs (523 and 697 nm) follow the TR as it is affected by the potassium treatment which make them most sensitive to TR and the different treatments.

Accordingly, the optimal time window for spectral measurements may vary, inter alia, by the plant and its response to the ambient conditions.

The high spectral and spatial resolution of the imaging spectroscopy system, generated by the proximity of the sensor to the plant canopy, provided a detailed and inclusive mean canopy spectrum based on hundreds to thousands of pixels from each plant. The disadvantage of this measurement setup is that the images are difficult to interpret once the plants' canopies overlap. There is always a tradeoff between the sample size for each treatment and the length of the period of hyperspectral imaging. However, in this study a larger sample size with a relatively short imaging period proved to have an advantage, as several plants were infected with root fungi and had to be removed from the analysis. Using this system in a different setup, e.g., other plant species and number of plants, it is important to consider the tradeoffs and plan accordingly. For instance, tomato plants grow much wider and must be placed farther apart so that the research hypothesis can be fully investigated, and a binary mask must be selected accordingly (i.e., to be able to monitor non chlorophyll dominant leaves).

Nonetheless, the current experiment, during which the plants' growth rate was monitored continuously, provided an extended insight to the effects of potassium application on plants' biomass gain and spectral response. The PA system indicated that, even in cases where daily transpiration and daily mass gain were not significantly different, the TR values were substantially different between plants of different treatments during several hours of the day. This implies that different energy balance and water utilization strategies have been used by the plants in different treatment groups to achieve a similar biomass gain during the period of spectral measurements in parallel to the physiological measurements. Consequently, the decision when to image the plants for the purpose of linking the spectral data to a physiological trait, such as TR, is not straightforward.

Traditionally, remote sensing of vegetation was carried out using a portable field spectrograph scanning the canopy reflectance. Furthermore, plant point spectroscopy is carried out on selected detached leaves in the laboratory or in the field using a leaf scanning apparatus [30]. Leaf or canopy spectral measurements are normally only conducted several times during a growing experiment, between 11:00 and 14:00, when the illumination is strongest. These measurements are time-consuming and labor-intensive, meaning that in order to measure large sample sizes, such as in this experiment, as well as measure supporting physiological data such as TR, 3–5 h should be reserved. In addition, the contact between the leaf and the spectrometer's fore optics might damage the leaf cuticle and render a natural response. The ability to measure an entire array of plants spectrally and physiologically using the hybrid system without an artificial lighting overcomes these obstacles. Moreover, the measurements are usually not coupled, and the time between the different sets of measurements can affect the plant's physiology and varying ambient conditions. During this time, the plant TR may vary substantially, and the experimental results may be biased. In addition, the results from this experiment show that a set of measurements between the hours of 11:00–13:00 would result in biased and misleading differences (spectrally) and nonsignificant differences (physiologically) between treatments, rendering the spectral measurements useless for this purpose.

Plant TR follows a daily cyclic pattern (Figure 6), influenced by the changing photosynthetic active radiation, relative humidity, and vapor pressure deficit. Using the hybrid PA with an imaging spectroscopy sensor may have some disadvantages, such as during cloud overpass, which affects the quality of the images and the coupling to co-acquired physiological data. However, since TR values were averaged over 15 min before and after every image acquisition, and white reference calibration prior to each image acquisition, the effects of passing clouds and changing sun conditions on plant TR were reduced.

Potassium is considered a macro-element in the plant and is responsible for diverse physiological functions, such as photosynthesis regulation, enzyme activation, protein synthesis, osmoregulation, and stomatal regulation [31]. Potassium deficit affects the guard cell and stomatal closure, which presumebly results with higher transpiration. In addition, potassium surplus may greatly reduce grain loss caused by restricted irrigation [32]. Although no daily transpiration differences were found

between the treatment groups, a higher TR was evident during the morning period for the potassium deficit treatment and a smaller TR during the afternoon, while surplus potassium had a significant effect on the TR only during the morning.

Even though the plants were under different potassium treatments, water was not limited. As such, an expected effect of potassium on the spectral absorption features at 950–970 nm that is known to be correlated with plant water concentration was not evidant [29,33]. Given that the NIR reflectance of leaves displays very little absorption and is mainly affected by the light scattering of the cell's inner structure and thickness [34], it was expected that NIR reflectance would be highly correlated with the addition or retraction of potassium from the plants. TR varied between the groups at different hours, which is captured in the spectra and in the ability to analyze the spectra and its correlations by the time of the day. In addition, as most greenhouse phenomics systems do not allow plants to flower and embalm, the current system favors that, paving the path to not only monitoring the plant in its early growing stages, but also predicting its final biomass gain and crop yield. Additional plant species and physiological attributes may be exploited by this system and presumably modeled to aid fertigation throughout the growing period. A look-up table of every plant may assist field remote sensing operators to focus on the best timing to answer different questions related to nutrition deficiency, water stress, and other physiological threats.

5. Summary and Conclusions

A new hybrid hyperspectral-physiological phenomics system was presented, which captured hourly hyperspectral images of a large array of plants under controlled conditions in a greenhouse. The images were supported by physiological measurements on computerized weighing lysimeters. This combination facilitated the study of the relationship between the spectral and physiological responses of the plants under potassium treatments, particularly TR. The ability to correlate the hourly spectral information to the changes in TR was exploited by calculating NDIs which varied throughout the day. The ability to capture differences in momentary TR, resulting from administered potassium treatment, using spectral information is highly depended on the time of measurement. Furthermore, in future systems, the plants' arrangement and the field of view of the spectral imaging sensor can be improved to capture larger areas that will enable larger distances between the pots to prevent canopy overlap. Additionally, using the NDIs in combination with TR for pepper plants in this experiment revealed that noon is not necessarily the best time to perform remote sensing measurements. Conversely, the afternoon and a set of specific NDI (523, 697 and 816 nm) is the best time to combine spectral and physiological measurements to discriminate low and high potassium fertilization in pepper plants under greenhouse conditions. This paves the path for additional research on other types of plants with nutrient deficiencies and abiotic stress. While this research was a proof of concept to the hybrid system concept—focused on an exploratory analysis of the system's abilities—future work with similar systems should focus on different fertilizers and abiotic stress induction to explore new insights to daily plant physiological and spectral changes.

References

1.   Furbank, R.T.; Tester, M. Phenomics – technologies to relieve the phenotyping bottleneck. *Trends Plant Sci.* **2011**, *16*, 635–644. [CrossRef] [PubMed]
2.   United Nation—World Population Prospects. 2019. Available online: http://www.unpopulation.org (accessed on 1 March 2020).
3.   Furbank, R.T. Plant phenomics: From gene to form and function Robert. *Funct. Plant Biol.* **2009**, *36*, 1006–1015.
4.   White, J.W.; Andrade-sanchez, P.; Gore, M.A.; Bronson, K.F.; Coffelt, T.A.; Conley, M.M.; Feldmann, K.A.; French, A.N.; Heun, J.T.; Hunsaker, D.J.; et al. Field Crops Research Field-based phenomics for plant genetics research. *Field Crop. Res.* **2012**, *133*, 101–112. [CrossRef]
5.   Gosa, S.C.; Lupo, Y.; Moshelion, M. Quantitative and comparative analysis of whole-plant performance for functional physiological traits phenotyping: New tools to support pre-breeding and plant stress physiology studies. *Plant Sci.* **2018**, *282*, 49–59. [CrossRef]
6.   Rundquist, D.; Perk, R.; Leavitt, B.; Keydan, G.; Gitelson, A. Collecting spectral data over cropland vegetation using machine-positioning versus hand-positioning of the sensor. *Comput. Electron. Agric.* **2004**, *43*, 173–178. [CrossRef]
7.   Ren, P.; Meng, Q.; Zhang, Y.; Zhao, L.; Yuan, X.; Feng, X. An Unmanned Airship Thermal Infrared Remote Sensing System for Low-Altitude and High Spatial Resolution Monitoring of Urban Thermal Environments: Integration and an Experiment. *Remote Sens.* **2015**, 14259–14275. [CrossRef]
8.   Chapman, S.; Hrabar, S.; Chan, A.; Dreccer, M.; Holland, E.; Ling, T.; Zheng, B.; Jackway, P.; Merz, T.; Jimenez-Berni, J. Pheno-Copter: A Low-Altitude, Autonomous Remote-Sensing Robotic Helicopter for High-Throughput Field-Based Phenotyping. *Agronomy* **2014**, *4*, 279–301. [CrossRef]
9.   Siebers, M.H.; Edwards, E.J.; Salim, M.; Walker, R.R. Fast Phenomics in Vineyards: Development of GRover, the Grapevine Rover, and LiDAR for Assessing Grapevine Traits in the Field. *Sensors* **2018**, *18*, 2924. [CrossRef]
10. Bai, G.; Ge, Y.; Hussain, W.; Baenziger, P.S.; Graef, G. A multi-sensor system for high throughput field phenotyping in soybean and wheat breeding. *Comput. Electron. Agric.* **2016**, *128*, 181–192. [CrossRef]
11. Ge, Y.; Bai, G.; Stoerger, V.; Schnable, J.C. Temporal dynamics of maize plant growth, water use, and leaf water content using automated high throughput RGB and hyperspectral imaging. *Comput. Electron. Agric.* **2016**, *127*, 625–632. [CrossRef]
12. Pandey, P.; Ge, Y.; Stoerger, V.; Schnable, J.C. High Throughput In vivo Analysis of Plant Leaf Chemical Properties Using Hyperspectral Imaging. *Front. Plant Sci.* **2017**, *8*, 1–12. [CrossRef] [PubMed]
13. Roitsch, T.; Cabrera-Bosquet, L.; Fournier, A.; Ghamkhar, K.; Jiménez-Berni, J.; Pinto, F.; Ober, E.S. Review: New sensors and data-driven approaches—A path to next generation phenomics. *Plant Sci.* **2019**. [CrossRef] [PubMed]
14. Elvanidi, A.; Katsoulas, N.; Ferentinos, K.P.; Bartzanas, T.; Kittas, C. Hyperspectral machine vision as a tool for water stress severity assessment in soilless tomato crop. *Biosyst. Eng.* **2018**, *165*, 25–35. [CrossRef]
15. Pacumbaba, R.O.; Beyl, C.A. Changes in hyperspectral reflectance signatures of lettuce leaves in response to macronutrient deficiencies. *Adv. Sp. Res.* **2011**, *48*, 32–42. [CrossRef]
16. Hulley, G.; Hook, S.; Fisher, J.; Lee, C. ECOSTRESS, A NASA Earth-Ventures Instrument for studying links between the water cycle and plant health over the diurnal cycle. *Int. Geosci. Remote Sens. Symp.* **2017**, *2017*, 5494–5496.
17. Gamon, A.; Pe uelas, J.; Field, C.B. A narrow-waveband spectral index that tracks diurnal changes in photosynthetic efficiency. *Remote Sens. Environ.* **1992**, *41*, 35–44. [CrossRef]
18. Halperin, O.; Gebremedhin, A.; Wallach, R.; Moshelion, M. High-throughput physiological phenotyping and screening system for the characterization of plant–environment interactions. *Plant J.* **2017**, *89*, 839–850. [CrossRef]
19. Dalal, A.; Bourstein, R.; Haish, N.; Shenhar, I.; Wallach, R.; Moshelion, M. Dynamic Physiological Phenotyping of Drought-Stressed Pepper Plants Treated With "Productivity-Enhancing" and "Survivability-Enhancing" Biostimulants. *Front. Plant Sci.* **2019**, *10*. [CrossRef]
20. Underwood, J.; Wendel, A.; Schofield, B.; Mcmurray, L.; Kimber, R. Efficient in-field plant phenomics for row-crops with an autonomous ground vehicle. *Field Robot.* **2017**, *34*, 1061–1083. [CrossRef]

21. Biddington, N.L. The effects of mechanically-induced stress in plants-a review. *Plant Growth Regul.* **1986**, *4*, 103–123. [CrossRef]

22. Vora, P.L.; Farrell, J.E.; Tietz, J.D.; Brainard, D.H. Image capture: Simulation of sensor responses from hyperspectral images. *IEEE Trans. Image Process.* **2001**, *10*, 307–316. [CrossRef] [PubMed]

23. Walczykowski, P.; Siok, K.; Jenerowicz, A. Methodology for determining optimal exposure parameters of a hyperspectral scanning sensor. *Int. Arch. Photogramm. Remote Sens. Spat. Inf. Sci. ISPRS Arch.* **2016**, *2016*, 1065–1069. [CrossRef]

24. Otsu, N. A Tlreshold Selection Method from Gray-Level Histograms. *IEEE Trans. Syst. Man Cybern.* **1979**, *C*, 62–66. [CrossRef]

25. Savitzky, A.; Golay, M.J.E. Smoothing and Differentiation of Data by Simplified Least Squares Procedures. *Anal. Chem.* **1964**, *36*, 1627–1639. [CrossRef]

26. Barnes, R.J.; Dhanoa, M.S.; Lister, S.J. Standard Normal Variate Transformation and De-Trending of Near-Infrared Diffuse Reflectance Spectra. *Appl. Spectrosc.* **1989**, *43*, 772–777. [CrossRef]

27. Corder, G.W.; Foreman, D.I. *Nonparametric Statistics for Non-Statisticians: A Step-by-Step Approach*; Wiley: Hoboken, NJ, USA, 2011; ISBN 9781118165881.

28. Gao, B.-C. NDWI A Normalized Difference Water Index for Remote Sensing of Vegetation Liquid Water From Space. *Remote Sens. Environ.* **1996**, *7212*, 257–266. [CrossRef]

29. Curran, P.J. Remote sensing of foliar chemistry. *Remote Sens. Environ.* **1989**, *30*, 271–278. [CrossRef]

30. Rapaport, T.; Hochberg, U.; Rachmilevitch, S.; Karnieli, A. The Effect of Differential Growth Rates across Plants on Spectral Predictions The Effect of Differential Growth Rates across Plants on Spectral Predictions of Physiological Parameters. *PLoS ONE* **2014**, *9*, e889. [CrossRef]

31. Marschner, H.; Marschner, P. *Marschner's Mineral Nutrition of Higher Plants*; Academic Press: Cambridge, MA, USA, 2012; ISBN 9780123849052.

32. Cakmak, I. The role of potassium in alleviating detrimental effects of abiotic stresses in plants. *J. Plant Nutr. Soil Sci.* **2005**, *168*, 521–530. [CrossRef]

33. Penuelas, J.; Filella, I.; Biel, C.; Serrano, L.; Save, R. The reflectance at the 950-970 nm region as an indicator of plant water status. *Int. J. Remote Sens.* **1993**, *14*, 1887–1905. [CrossRef]

34. Tucker, C.J. Remote sensing of leaf water content in the near infrared. *Remote Sens. Environ.* **1980**, *10*, 23–32. [CrossRef]